SIAM J. Applied Dynamical Systems
Vol. 7, No. 3, pp. 766–794

On Synchronization and Traveling Waves in Chains of Relaxation Oscillators with an Application to Lamprey CPG*

Péter L. Várkonyi† and Philip Holmes‡

Abstract. We study chains of relaxation-type neural oscillators with local excitatory coupling. Phase reductions suggest that such networks typically exhibit traveling waves, but relaxation oscillators often synchronize. We examine these behaviors using the phase response and fast threshold modulation (FTM) theories, which respectively describe network behavior for infinitesimally weak and moderate coupling. Surprisingly, the two different approximations yield quantitatively consistent predictions for chains with one-way coupling. Specifically, approaching the relaxation limit, such chains can exhibit waves with vanishing phase differences (i.e., synchrony) propagating in the coupling direction, *or* waves with persistent phase differences traveling against the coupling direction. These results provide novel support for the finding that caudo-rostral coupling dominates in the lamprey central pattern generator (CPG), and they suggest that recent models may underestimate the role of network effects in burst generation.

Key words. fast threshold modulation, phase reduction, relaxation oscillators, synchronization, traveling waves

AMS subject classifications. 34C26, 34C15, 34C29

DOI. 10.1137/070710329

1. Introduction.

Phase reduction theory, originally developed by Malkin [30, 31] and independently rediscovered by Winfree [43] (cf. [14]), provides a method for the simplification and analysis of networks of coupled oscillators, including those composed of spontaneously oscillatory spiking or bursting neurons. Augmented by the averaging theorem [15] for weakly coupled systems, it allows one to reduce N sets of M ordinary differential equations (ODEs), each set describing an oscillator having a hyperbolic (attracting) limit cycle, to a system of N ODEs approximating the phases of each oscillator along its limit cycle. See [18] and [19] for more recent statements of Malkin's theorem. Phase reduction always applies for sufficiently weak coupling, but it often extends to stronger coupling [11].

According to this theory, chains of oscillators with local coupling generically exhibit traveling waves, except for symmetrical bidirectional coupling or special types of interactions such as coupling of neural oscillators via gap junctions [7, 22, 23]. However, the interaction of relaxation oscillators seems to be exceptional: they phase-lock with zero phase-difference,

*Received by the editors December 6, 2007; accepted for publication (in revised form) by D. Terman April 3, 2008; published electronically July 23, 2008. This work was partially supported by NSF EF-0425878 and NIH NS054271.

http://www.siam.org/journals/siads/7-3/71032.html

†Department of Mechanics, Materials and Structures, Budapest University of Technology and Economics, Müegyetem rkp. 3-9, H-1111 Budapest, Hungary (vpeter@mit.bme.hu). This author was supported by Imre Korányi and Zoltán Magyary fellowships as well as by OTKA-72368 and was hosted by the Program in Applied and Computational Mathematics of Princeton University.

‡Program in Applied and Computational Mathematics, and Department of Mechanical and Aerospace Engineering, Princeton University, Princeton, NJ 08544 (pholmes@math.princeton.edu).

(i.e., they synchronize) in cases where one would expect traveling waves [35, 36]. This synchrony is robust against perturbations: while phase oscillators compensate for perturbations by changing their phase relations, relaxation oscillators typically compensate via changes in waveforms.

There are at least two explanations for this behavior. Phase reduction neglects the effects of nonlinearities in coupling: it requires that orbits perturbed by coupling remain sufficiently close to unperturbed limit cycles at all times, which holds for *sufficiently weak* coupling $\epsilon \ll 1$. Relaxation oscillators combine fast and slow dynamics (i.e., two characteristic time-scales with ratio $\mu \ll 1$), and in this case phase reduction requires *extremely weak* coupling: $\epsilon \ll \mu$ [19]. In relevant ranges of μ, the oscillators' interactions are typically dominated by higher order effects that are not captured by phase theory. Fast threshold modulation (FTM) theory [35, 36] was introduced to explain this behavior. Motivated by synaptic coupling of neural oscillators, it applies to moderate or strong coupling: $\mu \ll \epsilon$.

Despite the apparent contrast between relaxation and phase oscillators, and the limited applicability of phase reduction to the former, phase theory can also account for synchronization of relaxation oscillators [19], and its predictions agree qualitatively with those of FTM theory. The reason for this unexpected behavior is that the function $H(\psi)$ describing the effect of coupling between two oscillators is discontinuous at certain points with respect to their phase difference ψ.

In this paper we apply phase reduction for weak coupling ($\epsilon \ll \mu \ll 1$) and a combination of FTM and phase theory for relaxation-type oscillators ($\mu \ll \epsilon \ll 1$). We ask if a given system exhibits traveling waves or synchrony and compare predictions of the two methods, thereby shedding light on behaviors expected under variations in coupling strength ϵ. Both approaches are required to obtain a global picture of the behavior of coupled chains, and we show that their predictions are *quantitatively* similar in chains with one-way coupling, despite the different mechanisms. In section 2 we analyze a pair of oscillators with one-way coupling in the phase reduction limit and outline a generalization to unidirectionally coupled oscillator chains, and section 3 is an analogous study of the FTM limit. In these sections we describe an interesting property of traveling wave solutions: in the limit $\mu \to 0$ waves propagating in the coupling direction approach synchronous dynamics, but counterpropagating waves persist (Theorems 2.1 and 3.1). These results provide quantitative conditions for traveling waves versus synchrony in arrays of unidirectionally coupled relaxation oscillators. The behavior of bidirectionally coupled chains is also briefly discussed at the end of each section. In section 4 we demonstrate that most, but not all, simple oscillators exhibit the first behavior: synchrony is more common in the relaxation limit than traveling waves, and we provide a sufficient condition for this in Theorem 4.1. Section 5 contains illustrative examples of both behaviors.

In section 6, we apply these results to the neural central pattern generator (CPG) of the lamprey. Recent lamprey CPG models [39, 27, 26] are double chains of relaxation-type bursters in which the burst frequency is adjusted by neuro-modulators that tune the slow time-scale μ so that the relaxation limit is approached as swimming speed decreases. Simulations indicate that these models exhibit synchrony in the relaxation limit and that phase lags between neighboring units depend strongly on swimming frequency, being small at low frequency and larger at high frequency. In contrast, the animal exhibits quasi–frequency-independent phase patterns. As we will show, this shortcoming could be eliminated if the model's parameters

were adjusted to generate traveling waves in the relaxation limit. The paper concludes with section 7. We relegate many technical details in the proofs of Theorems 2.1 and 3.1 to a series of appendices. Background on CPGs can be found in [8], and background on phase and relaxation oscillator models can be found in [21, 23].

2. Relaxation oscillators in the phase limit. We consider a pair of identical relaxation oscillators O_1, O_2, each with one slow variable x_j and one fast one y_j. The time-scale ratio is set by the parameter $0 < \mu \ll 1$, and $\mu \to 0$ is the relaxation limit. If O_1 receives weak coupling ($\epsilon \ll \mu$) from O_2 in the fast variable, the ODEs for O_1 are

$$\dot{x_1} = f(x_1, y_1), \tag{2.1}$$

$$\dot{y_1} = \frac{1}{\mu}\left[g(x_1, y_1) + \epsilon h(x_1, y_1, x_2, y_2)\right], \tag{2.2}$$

while those of O_2 are the same, but without the coupling term h. Henceforth we assume that the fast equation (2.2) has a cubic-shaped nullcline or *slow manifold* $g = 0$, and that for $\epsilon = 0$ a stable hyperbolic limit cycle Γ of period T exists, on which x_j slowly decreases (resp., increases) near the lower (resp., upper) branch of $g = 0$; see Figure 1. Henceforth, in describing a single oscillator, we typically drop the subscripts.

In section 2.1 we summarize the results of Izhikevich [19] and prepare for section 2.2. There we prove our first theorem, extending the leading order phase response curve (PRC) expressions of [19] to the next order and providing explicit estimates of the width and height of PRC peaks in terms of fractional powers of μ (Figure 5).

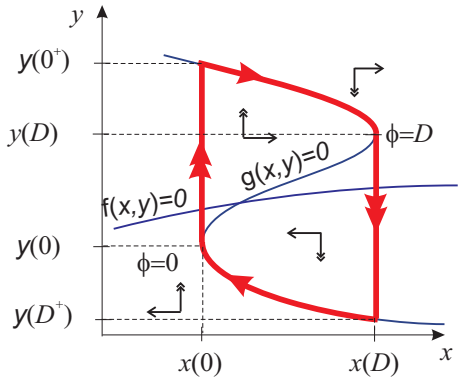

Figure 1. *Schematic phase portrait of a 2D relaxation oscillator with cubic-shaped nullcline (thin curve). Arrows show directions of the vectorfield; ϕ denotes the phase along the limit cycle (thick curve); $\phi = 0, D$ denote phase values at the instantaneous jumps; and $x(0)$, $y(0)$, $y(0^+)$, etc. denote the coordinates of the corresponding points in phase space. Oscillators are assumed to be active on the upper branch $\phi \in (0, D)$ and silent on the lower branch $\phi \in (D, 0)$.*

2.1. Phase reduction and previous results. Like any ODE with a stable hyperbolic limit cycle, (2.1)–(2.2) can be reduced to a phase description [18]. We define the phase $\phi = \phi(x, y)$ along Γ such that the periodic solution satisfies $\dot{\phi} = 2\pi/T \stackrel{\text{def}}{=} \omega$, and we let $x(\phi)$, $y(\phi)$, etc. denote coordinates of points on Γ. The system of four coupled ODEs may then be

reduced to the phase equations

$$\dot{\phi_1} = \omega + \frac{\epsilon}{\mu}\tilde{h}(\phi_1, \phi_2)z(\phi_1) + \mathcal{O}(\epsilon^2), \quad \dot{\phi_2} = \omega, \tag{2.3}$$

where $\tilde{h}(\phi_1, \phi_2) = h(x_1(\phi_1), y_1(\phi_2), x_2(\phi_2), y_2(\phi_2))$ denotes the coupling function evaluated on Γ. Here the PRC $z(\phi)$ represents the sensitivity of O_1 to perturbations from O_2, and $z(\phi) > 0$ (resp., $z(\phi) < 0$) means that an excitatory signal ($h > 0$) received at $(x(\phi), y(\phi))$ speeds up (resp., slows down) O_1. In deriving the PRC one expands about Γ in a Taylor series, thereby neglecting nonlinear ($O(\epsilon^2)$) coupling effects. See [10, 3] for recent examples of explicit PRC computations.

After introducing the phase difference $\psi = \phi_1 - \phi_2$, (2.3) can be averaged over the period T and subtracted to yield

$$\dot{\psi} = \frac{\epsilon}{2\pi\mu}\int_0^{2\pi} \tilde{h}(\varphi + \psi, \varphi)z(\varphi + \psi)\, d\varphi + O(\epsilon^2) \stackrel{\text{def}}{=} H(\psi) + O(\epsilon^2). \tag{2.4}$$

Zeros of H correspond to phase differences at which the oscillators phase-lock ($\psi = \text{const}$), and stable phase-locking occurs if $H(\psi) = 0$ and $dH(\psi)/d\psi < 0$. For details, see [18, 17].

While in general PRCs must be computed numerically, in [19, section 2] analytical formulae were derived for (2.1)–(2.2) in the limit $\mu \to 0$, as follows. Let $z^*(\phi) \stackrel{\text{def}}{=} z(\phi)/\mu$; subscripts x and y denote partial derivatives, $\phi^{(1)} = 0$ and $\phi^{(2)} = D$ denote phase values at the jumps, $y(\phi^{(j)}) = y(0), y(D)$ denote the value of y immediately before a jump, and $y(\phi^{(j)+}) = y(0^+), y(D^+)$ denotes its value immediately after it (Figure 1). If $\phi \neq \phi^{(j)}$, $j \in \{1, 2\}$, then

$$z^*(\phi) = -\frac{\omega f_y(x(\phi), y(\phi))}{f(x(\phi), y(\phi))g_y(x(\phi), y(\phi))}, \tag{2.5}$$

and near the jumps $\phi = \phi^{(j)}$,

$$z^*(\phi) = \frac{\delta(\phi - \phi^{(j)})\,\omega^2}{g_x(x(\phi^{(j)}), y(\phi^{(j)}))}\left[\frac{1}{f(x(\phi^{(j)}), y(\phi^{(j)}))} - \frac{1}{f(x(\phi^{(j)}), y(\phi^{(j)+}))}\right]. \tag{2.6}$$

Equation (2.5) follows from linearization in the neighborhood of the slow parts of Γ on the upper and lower branches of the $g = 0$ nullcline, and it may be derived from the adjoint formulation of the PRC [18], as in [19, (2.9)]. Equation (2.6) is found by considering the jumps from $y(0)$ to $y(0^+)$ and $y(D)$ to $y(D^+)$ (Figure 1; cf. [19, (2.4)]). The delta functions at $\phi^{(j)}$ play a central role in explaining the behavior of coupled relaxation oscillators; see Figure 2.

To formulate our results, we supplement (2.5)–(2.6) with the following conditions:

(i) The coupling term $h \equiv 1$ while O_2 is near the upper branch of its $g = 0$ nullcline (for $\mu \to 0$ this implies $\phi \in (0, D)$), and $h \equiv 0$ near the lower branch. During jumps, $0 \leq h \leq 1$.

(ii) $\partial f(x, y)/\partial y > 0$ at arbitrary points $(x(\phi), y(\phi))$ along the limit cycle.

(iii) The duty cycle $D/(2\pi) \leq 0.5$ (time spent on the upper (active) branch is not more than that spent on the lower branch).

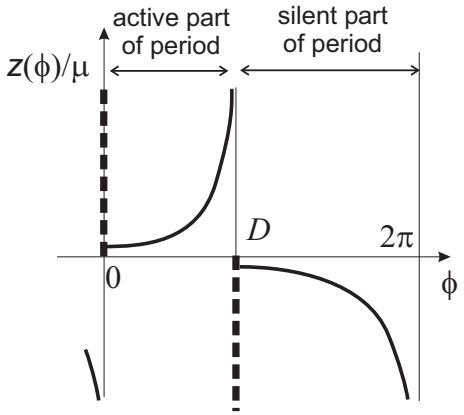

Figure 2. *Schematic PRC for a relaxation oscillator in the limit $\mu \to 0$ as derived in* [19]. *The function has singularities and delta functions (thick dashed lines) at $\phi = 0, D$. The sign of the delta functions is always as shown. The sign of the continuous parts is as shown if condition* (ii) *holds.*

Condition (i) simplifies the notion that oscillators have active (e.g., bursting) and silent (e.g., refractory) states; it has been used by other authors (e.g., [35, 36, 19]). Condition (ii) requires that $f(x, y)$ is strictly monotonic in y, which is true for most oscillator models, and it implies that the sign of z^* is as shown in Figure 2, due to the following facts:

(1) On the limit cycle of Figure 1, $f(x(0), y(0)) < 0$, $f(x(0), y(0^+)) > 0$, and $g_x(x(0), y(0)) < 0$, so (2.6) implies that the peak in z^* at $\phi = 0$ is positive. Similarly, the peak at $\phi = D$ is negative.

(2) Attractivity of the upper and lower branches of the $g = 0$ nullcline implies that $g_y < 0$; $f > 0$ on the upper branches and $f < 0$ on the lower branches, and $f_y > 0$, by condition (ii). Thus (2.5) gives positive and negative PRC values during the active and silent parts of the limit cycle, respectively.

Under condition (i), (2.4) simplifies to

$$H(\psi) = \frac{\epsilon}{2\pi} \int_{\psi}^{D+\psi} z^*(\phi)\, d\phi; \tag{2.7}$$

the resulting function $H(\psi)$ is shown in Figure 3, in which its key properties are also summarized. In particular, H is discontinuous: when $\phi^{(i)}$ enters or leaves the interval of integration $[\psi, D + \psi]$ in (2.7), the delta functions in (2.6) introduce step changes. If the decreasing step at $\psi = 0$ passes through 0, then $H(\psi)$ has a root at 0, corresponding to synchronization, which is robust against perturbations such as adding a constant to H. This fact was advanced in [19] to explain why weakly coupled relaxation oscillators tend to synchronize.

Note that the properties of $H(\psi)$ shown in Figure 3 require condition (iii); for $D > \pi$, H may have arbitrarily many roots or possibly none at all. Condition (iii) holds for the majority of important relaxation oscillators, and it appears elsewhere in the literature [24]. We also remark that, since $\lim_{\phi \to \phi^{(i)}} g_y = 0$ and $g_y \backsim (\phi^{(i)} - \phi)^{1/2}$, the rescaled PRC $z^*(\phi)$ in (2.5) has integrable singularities at $\phi = \phi^{(j)}$.

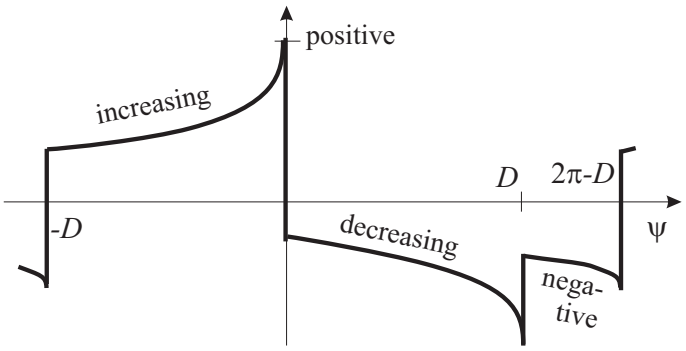

Figure 3. *Schematic coupling function $H(\psi)$ for a relaxation oscillator with weak one-way coupling in the limit $\epsilon \ll \mu \to 0$, as derived in* [19]. *If conditions* (i)–(iii) *hold, the qualitative form of H and the directions of the steps are as shown.*

2.2. Phase-locking and synchrony. While the discontinuity of H at $\psi = 0$ often yields synchronization, this is not the only possibility: if $\text{sign}(H(0^+)) = \text{sign}(H(0^-))$, the oscillators do not synchronize, although phase-locking can occur at $\psi \neq 0$ if H has nonzero roots. This latter case corresponds to traveling waves in a chain (see section 2.3). Here we state a result that shows that phase-locked solutions with $\psi = \Delta(\mu) \leq 0$ behave differently from those with $\Delta(\mu) > 0$, thereby distinguishing the two behaviors.

Theorem 2.1. *Let $H_\mu(\psi)$ denote the averaged coupling function at a given value of μ, and let $(x, y) = (\xi, \upsilon(\xi))$ denote the equation of the active branch of the slow manifold. Assume that the phase-shift $\Delta(\mu)$ satisfies $dH_\mu(\psi)/d\psi|_{\Delta(\mu)} < 0 = H_\mu(\Delta(\mu))$.*

(a) *If conditions* (i)–(iii) *hold and*

$$-\int_{x(0)}^{x(D)} \frac{f_y(\xi,\upsilon(\xi))}{f^2(\xi,\upsilon(\xi))g_y(\xi,\upsilon(\xi))}\,d\xi + \frac{1}{g_x(x(D),y(D))}\left[\frac{1}{f(x(D),y(D))} - \frac{1}{f(x(D),y(D+))}\right] > 0, \tag{2.8}$$

then $0 < \lim_{\mu\to 0}\Delta(\mu) < \pi$; i.e., O_1 leads O_2.

(b) *If conditions* (i)–(iii) *hold and* (2.8) *is false, then $\Delta(\mu) \backsim -\mu^{2/3}$ for small μ and $\lim_{\mu\to 0}\Delta(\mu) = 0$; i.e., the oscillators synchronize.*

Proof. We extend the results of [19] to the case $0 < \mu \ll 1$. The limit cycle consists of three parts, known in singular perturbed and boundary layer theory as the outer, inner, and intermediate limits [2]; see Figure 4.

1. Evolution along slow manifolds: These episodes occupy time $O(1)$, and the PRCs are well approximated by (2.5); thus $z^*(\phi) = O(1)$.
2. Transition from slow motion to jumps at the knees of the $g = 0$ nullcline: These take time $O(\mu^{2/3})$ [2], and, as shown below, the phase response converges to (2.6) in the relaxation limit; thus $z^*(\phi) = O(\mu^{-2/3})$.
3. Fast jumps of duration $O(\mu)$ between slow manifolds: Here $z^*(\phi) = O(1)$, as in case 1.

These statements follow from the arguments of [19], summarized in section 2.1, with the crucial additional fact, shown in Appendix A, that the delta function in (2.6) derives from

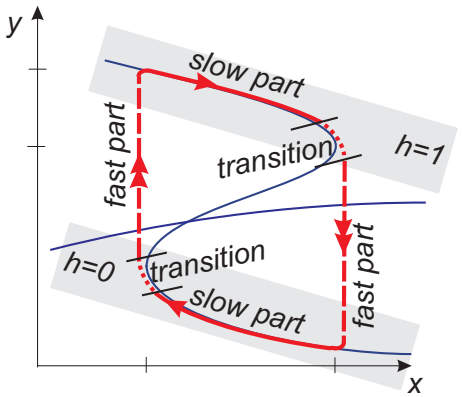

Figure 4. *Characteristic segments of the limit cycle of a relaxation oscillator: Slow motion along nullclines, fast jumps, and transition. Coupling h is assumed constant ($\equiv 0$ or 1) near the slow nullclines, shown shaded.*

perturbations during transition and *not* during the fast jump. Intuitively, perturbations can advance the jump as solutions approach the fold, but perturbations in the fast variable have little effect during the jump ($z \backsim O(\mu)$, i.e., $z^* \backsim O(1)$), due to the $O(\mu^{-1})$ speed of the dynamics. The resulting PRC is shown in Figure 5.

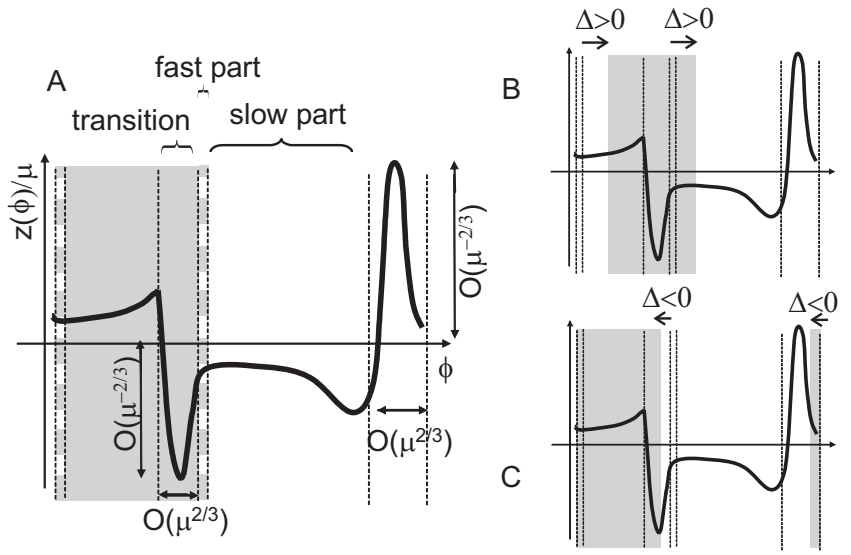

Figure 5. A: *PRCs for relaxation oscillators with $0 \neq \mu \ll 1$. Grey denotes the active part of the period $h \equiv 1$, white the silent part $h \equiv 0$, and striped, far from the nullclines, h not defined by condition* (i). *For synchrony, $H(0)$ is the integral of z^* over the grey interval.* B: *For small $\psi > 0$, $H(\psi)$ is the integral over a domain shifted rightward compared to the case $\psi = 0$.* C: *For small $\psi < 0$, the integration domain is shifted leftward and includes the peaks of z^*.*

If the two oscillators are in synchrony ($\psi = 0$), O_1 receives a coupling signal during both the slow and transitional parts near the *upper nullcline* according to condition (i); there is no input during slow and transition parts near the lower nullcline. Condition (i) does not

determine h during the fast jumps, since the state is far from both nullclines. However, the integral of z^* during these episodes is only $O(\mu)$ ($\sim$ the jump duration), so its contribution to H vanishes as $\mu \to 0$; cf. (2.7). Thus, if μ is sufficiently close to 0, $H_\mu(0)$ is well approximated by the integral of z^* over the slow and transition parts on the upper branch, and using (2.5)–(2.7), we obtain

$$H_\mu(0) = \frac{\epsilon\omega^2}{2\pi}\left[\int_0^D \frac{-f_y(x(\phi),y(\phi))}{\omega f(x(\phi),y(\phi))g_y(x(\phi),y(\phi))}\,d\phi \right. \\ \left. + \frac{1}{g_x(x(D),y(D))}\left(\frac{1}{f(x(D),y(D))} - \frac{1}{f(x(D),y(D^+))}\right)\right] + \mathcal{O}(\mu); \tag{2.9}$$

see also Figure 5(A).

Due to (2.1) and (2.3), we have $d\phi = dx \cdot \omega/f$; hence (2.9) is equal to the left-hand side of (2.8) modulo the $O(\mu)$ term and the $\epsilon\omega^2/2\pi$ factor. Thus, case (a) of Theorem 2.1 corresponds to $\lim_{\mu\to 0} H_\mu(0) > 0$. If $\psi = 0$ at $t = 0$, ψ increases according to (2.4), and the limits of integration in (2.7) must be moved rightward to locate a zero of $H(\psi)$, as in Figure 5(B). At that point the limits do not intersect the peaks of the PRC, implying that H has finite slope just above $\psi = 0$. The conclusion of part (a) follows from this fact.

On the other hand, if $H(0) < 0$, the domain of integration must be shifted to the left and will intersect the PRC's peaks; see Figure 5(C). A negative peak of width $O(\mu^{2/3})$ and slope $O(\mu^{-2/3})$, which shrinks to a vertical step in the relaxation limit of Figure 2, lies just below $\psi = 0$. $\Delta(\mu)$ cannot lie elsewhere than at this steep part, since conditions (i)–(iii) imply that at all other points $H(\psi)$ is either negative or increasing; see Figure 3. ■

We remark that if only condition (i) holds, we still have $\lim_{\mu\to 0}\Delta(\mu) \neq 0$ in case (a). In case (b), conditions (i)–(ii) without (iii) imply the existence of the synchronous solution but do not imply its uniqueness. Condition (i) without (ii)–(iii) means that the oscillators often but not always synchronize.

2.3. Oscillator chains in the phase reduction limit. The behavior of coupled pairs of phase oscillators generalizes to that of chains. Here we review basic results based on [22, 25] and outline some consequences of Theorem 2.1.

Consider a chain of n identical oscillators. For one-way nearest-neighbor coupling and if $H(\psi)$ crosses 0, phase differences between adjacent oscillators are equal to those between a coupled pair, being determined by the stable zeros of H. For two-way coupling ($H_1(\psi)$ and $H_2(\psi)$) in a long chain ($n >> 1$), one direction is typically dominant and phase relations are unaffected by connections in the other, except near boundaries. In special cases (e.g., $H_1 \approx H_2$) neither direction dominates and phase differences may be nonuniform. If the coupling is translation-symmetric and close but not necessarily adjacent oscillators are coupled, then the chain mimics the behavior of a reduced network with nearest-neighbor connections.

Thus, our analysis of a pair of units also explains the behavior of a wide class of chains. Case (a) of Theorem 2.1 ($0 < \lim_{\mu\to 0}\Delta(\mu) < \pi$) means that the unit that receives coupling is advanced in phase compared to the other. Analogously, a chain exhibits traveling waves propagating against the coupling direction (against the dominant direction for two-way coupling), and, according to the theorem, such traveling waves persist in the relaxation limit $\mu \to 0$. In contrast, case (b) corresponds to a phase lag of the unit receiving coupling that vanishes

in the relaxation limit. The corresponding phenomenon in chains is a traveling wave that propagates in the (dominant) coupling direction and approaches synchrony in the relaxation limit.

3. Relaxation oscillators in the FTM limit. We again consider the system (2.1)–(2.2), but now under the assumption $\mu \ll \epsilon \ll 1$. FTM theory describes the interaction of relaxation oscillators that exhibit sufficiently fast jumps simultaneously ($\mu \ll \epsilon$). It neglects interactions during the periods of slow dynamics, so most FTM results have been qualitative in nature. Here we augment these results by combining FTM with phase reduction theory, assuming $\epsilon \ll 1$ so that the latter applies except near jumps. We retain the notation of section 2 with phase ϕ along the unperturbed limit cycle Γ and $(x(\phi), y(\phi))$ denoting points in the phase plane.

3.1. FTM theory. FTM theory and the synchronization of relaxation oscillators are described in detail in [35] via the example of a mutually coupled pair. (Chains and other networks are considered in [36].) Here we perform a similar analysis of a pair with one-way coupling.

Since ϵ is large compared to μ, we consider an unperturbed limit cycle ($h \equiv 0$) and a separate, perturbed limit cycle for $h \equiv 1$; see Figure 6(A). Since O_2 receives no coupling signal it follows the former. Input to O_1 is either 1 or 0, depending on the state of O_2, so O_1 intermittently switches between the two cycles. Jumps are assumed to be instantaneous. (In phase reduction, one considers only the unperturbed limit cycle, but "jumps" are not instantaneous.)

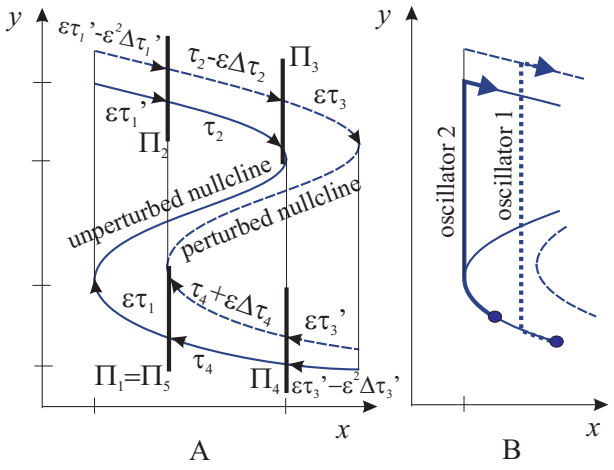

Figure 6. A: *Unperturbed (solid) and perturbed (dashed) nullclines.* Π_i *and* τ_i *represent Poincaré sections and times required to pass certain trajectories, respectively, as used in Appendix B.* B: *An example of FTM interaction:* O_2 *(solid) slightly leads* O_1 *(dashed); when* O_2 *jumps up,* O_1 *switches to the perturbed nullcline, leading to a synchronous jump.*

To illustrate FTM interaction, assume that the oscillators are almost synchronized and moving on the silent branch with O_1 slightly lagging behind O_2. When O_2 reaches the knee and jumps, it sends O_1 to the perturbed limit cycle, thereby causing a synchronous jump, after which O_1 takes the lead. See Figure 6(B). Similarly, synchronous jumps occur if O_1 slightly leads O_2 prior to jumping down. This typically results in rapid and robust synchronization.

The example shows that oscillators with FTM interaction can compensate for deviations from perfect synchrony by keeping fast jumps synchronous and modulating their locations. However, while FTM interactions at jumps act to synchronize the units, accumulating interactions during slow phases may shift them apart. The relative strength of the two effects determines whether synchronization occurs.

The fact that the phase equation (2.3) is not applicable near jumps is illustrated by the following example. Consider two impulsive perturbations, each of strength and duration $\mathcal{O}(\epsilon)$, delivered when O_1 is on the orbit segment of length $\epsilon\tau_1$ in Figure 6(A). Either one alone immediately moves the state to the upper branch, causing an $\mathcal{O}(\epsilon)$ phase change, large compared to its size of $\mathcal{O}(\epsilon^2)$ (strength $\times$ duration). However, if the impulses act successively, the second has an effect of only $\mathcal{O}(\epsilon^2)$. The implicit assumption of phase reduction theory, that successive perturbations are additive, is violated.

3.2. Phase-locking and synchrony. Examples like those above show that the notion of phase difference is unclear, so we introduce the following definitions to categorize different types of T-periodic interactions of pairs of oscillators under FTM:

(a) *Oscillator* O_j *leads* O_i if O_i is silent when O_j jumps up and O_i is active when O_j jumps down.

(b) *The oscillators alternate* if when either jumps up or down, the other is silent, or, alternatively, if when either jumps up or down, the other is active. Only the first case is possible under condition (iii).

(c) *The oscillators synchronize* if the time intervals that O_i spends in its active state are a subset of those spent by O_j in its active state or vice versa. This includes the case when jumps up and/or down are synchronous.

We can now state an analogue of Theorem 2.1.

Theorem 3.1. *Assume that two oscillators in the FTM limit ($\epsilon \to 0$, $\mu/\epsilon \to 0$) each have stable T-periodic solutions. Then*

(a) *if conditions* (i)–(iii) *and inequality* (2.8) *hold, O_1 leads O_2; and*

(b) *if conditions* (i)–(iii) *hold but inequality* (2.8) *does not, the oscillators synchronize.*

Proof. The lengthy proof is given in Appendix B. It relies primarily on defining a function H_{FTM}, analogous to H of section 2, which predicts the relative dynamics, and showing that H_{FTM} has the same shape in the limit $\epsilon \to 0$, $\mu/\epsilon \to 0$ as H does in the limit $\mu \to 0$, $\epsilon/\mu \to 0$. ■

In case (b) of Theorem 3.1 synchrony implies either that the jump in O_2 initiates an immediate jump in O_1 or that one of the oscillators jumps up earlier and jumps down later than the other. If there are synchronous jumps, it is intuitively clear that for small but nonzero μ this results in a small lag of the driven oscillator. Thus cases (b) of Theorems 2.1 and 3.1 are closely related. In contrast, if there is synchrony as defined above but no synchronous jumps, relations between the two theorems are less clear. However, in Appendix C we illustrate that the latter scenario is nongeneric for $\epsilon \to 0$.

There are some differences between the phase and FTM limits. For phase oscillators, $\Delta \backsim \mu^{2/3}$, as shown in Theorem 2.1(b). In the FTM case the $O(\mu)$ duration of fast jumps implies that $\Delta \backsim \mu$. We illustrate this by a numerical example in section 5.

3.3. Oscillator chains in the FTM case. As in phase response theory, the behavior of a unidirectionally coupled pair has implications for chains with one-way, nearest-neighbor coupling; i.e., in cases (a) and (b), chains typically exhibit traveling waves against and in the coupling direction, respectively, and in the relaxation limit synchrony results in case (b) but not in case (a). We suspect that more diffuse localized couplings can be reduced to the nearest-neighbor case, although we are unaware of specific studies of this type.

The behavior of chains FTM-coupled in both directions is less transparent than in case of phase-coupling. Oscillator pairs and arrays with *symmetrical* bidirectional FTM-coupling typically exhibit synchrony, and in contrast to phase-interaction, this is robust against perturbations of the coupling symmetry [35, 36]. These results indicate that asymmetrically coupled arrays (significantly stronger in one direction than in the other) are probably more likely to synchronize than those with unidirectional connections. Quantitative conditions for synchrony versus traveling waves for two-way coupling appear to be unknown. As we show in section 4, traveling wave behavior is much rarer than synchrony in one-way arrays. The above facts suggest that it is even rarer when connections in both directions are present.

4. Why do most oscillators synchronize? It was shown in sections 2 and 3 that oscillators can, but need not, synchronize in the relaxation limit $\mu \to 0$. As described in this section, we examined several simple two-dimensional relaxation oscillator models of neural oscillators and found that all exhibited synchrony. This suggests that inequality (2.8) of Theorem 2.1 is false for many examples. The following theorem provides a sufficient condition for this and hence for synchronization. Two oscillators satisfying conditions (i)–(iii) above and (iv) and (v) below always synchronize in the relaxation limit by Theorems 2.1 and 3.1.

Theorem 4.1. *Suppose that* (2.1)–(2.2) *satisfy condition* (ii)*, and additionally, at all points* (x, y) *on the "active" branch of the slow manifold* $g = 0$*, the following conditions hold.*

- *Condition* (iv): $f_x(x, y) \le 0$.
- *Condition* (v): $g_x(x, y) \le g_x(x(D), y(D))$.

Then inequality (2.8) *is false.*

Proof (by contradiction). The integral in (2.8) (or (2.9)) is evaluated along $g = 0$, on which an infinitesimal displacement $(d\xi, d\upsilon)$ satisfies

$$g_x(\xi, \upsilon)\, d\xi + g_y(\xi, \upsilon)\, d\upsilon = 0 \quad \text{or} \quad d\xi = -\frac{g_y(\xi, \upsilon)\, d\upsilon}{g_x(\xi, \upsilon)}. \tag{4.1}$$

We use (4.1) to change the variable of integration in (2.8) from ξ to υ, replacing $(\xi, \upsilon(\xi))$ by $(\xi(\upsilon), \upsilon)$, where $\xi(\upsilon)$ denotes the inverse of $\upsilon(\xi)$. Since $g_x < 0$ on the active nullcline, due to $g_x(x(D), y(D)) < 0$ and condition (v), this inverse is well defined in the case of interest. Inequality (2.8) becomes

$$\begin{aligned} &-\int_{y(D)}^{y(0+)} \frac{f_y(\xi(\upsilon), \upsilon)}{f^2(\xi(\upsilon), \upsilon) g_x(\xi(\upsilon), \upsilon)}\, d\upsilon \\ &+ \frac{1}{g_x(x(D), y(D))} \left[\frac{1}{f(x(D), y(D))} - \frac{1}{f(x(D), y(D^+))} \right] > 0. \end{aligned} \tag{4.2}$$

To show that (4.2) is false we first replace $g_x(x, y)$ in the integrand by the constant term $g_x(x(D), y(D))$, using the facts that $g_x(x, y) \le g_x(x(D), y(D)) < 0$ and $f_y < 0$ (condition (ii)),

which together imply that

$$\int_{y(D)}^{y(0+)} \frac{f_y(\xi(\upsilon),\upsilon)}{f^2(\xi(\upsilon),\upsilon)g_x(\xi(\upsilon),\upsilon)}\,d\upsilon \le \int_{y(D)}^{y(0+)} \frac{f_y(\xi(\upsilon),\upsilon)}{f^2(\xi(\upsilon),\upsilon)g_x(x(D),y(D))}\,d\upsilon.$$

We then multiply the resulting expression by the strictly positive quantity $-g_x(x(D),y(D))$ to deduce that, if (4.2) holds, then also

$$\int_{y(D)}^{y(0+)} \frac{f_y(\xi(\upsilon),\upsilon)}{f^2(\xi(\upsilon),\upsilon)}\,d\upsilon - \frac{1}{f(x(D),y(D))} + \frac{1}{f(x(D),y(D^+))} > 0,$$

which in turn implies that

$$\int_{y(D)}^{y(0+)} \frac{f_y(\xi(\upsilon),\upsilon)}{f^2(\xi(\upsilon),\upsilon)}\,d\upsilon - \frac{1}{f(x(D),y(D))} > 0, \tag{4.3}$$

where we use $1/f(x(D),y(D^+)) < 0$, since $f < 0$ on the "silent" branch of the slow manifold.

Next, using the chain rule and appealing to condition (iv) and the fact that $\xi(\upsilon)$ is a decreasing function, we have

$$\frac{df(\xi(\upsilon),\upsilon)}{d\upsilon} = f_y + f_x\frac{d\xi(\upsilon)}{d\upsilon} \ge f_y. \tag{4.4}$$

Equation (4.4) allows us to replace the partial derivative in the integrand of (4.3) by the total derivative and further to express it as an exact differential,

$$\int_{y(D)}^{y(0+)} \frac{df(\xi(\upsilon),\upsilon)/dy}{f^2(\xi(\upsilon),\upsilon)}\,d\upsilon = -f^{-1}(x_a(\upsilon),\upsilon)\big|_{y(D)}^{y(0+)}, \tag{4.5}$$

where $x_a(\upsilon)$ denotes points on the active branch and we use the fact that $(f^{-1})' = -f'/f^2$. Our inequality now reads

$$-f^{-1}(x_a(\upsilon),\upsilon)\big|_{y(D)}^{y(0+)} - \frac{1}{f(x(D),y(D))} = \frac{-1}{f(x(0),y(0+))} > 0. \tag{4.6}$$

But this is false, since $f(x,y) > 0$ on the active branch, providing our contradiction. ∎

Theorem 4.1 applies to many oscillator models with unidirectional coupling that satisfies condition (i). We analyzed the van der Pol oscillator [37] and neuron models of FitzHugh–Nagumo [12, 33], Hindmarsh–Rose [16], Morris–Lecar [32], and Rinzel [34], as well as a two-dimensional spike-rate description of the bursting half-center in the lamprey from [42, p. 209], obtaining the results summarized in Table 1. We also checked inequality (2.8) (in some cases numerically) and found that it was false in every case, in four of which Theorem 4.1 applies. This suggests that it is not easy to find relaxation oscillators that do not synchronize. Nonetheless, in the next section we provide an example of this apparently rare behavior.

Table 1

Evaluation of the applicability of conditions (ii)–(v) *and Theorem* 4.1 *for some simple oscillators. The * means yes for low values of input current, and no for high values.*

Model ODE	(ii)	(iii)	(iv)	(v)	Thm. 4.1 applies?	Thm. 2.1 predicts synchrony?
van der Pol	yes	yes	yes	yes	**yes**	**yes**
FitzHugh–Nagumo	yes	*	yes	yes	*****	**yes**
Hindmarsh–Rose	yes	yes	yes	yes	**yes**	**yes**
Morris–Lecar	yes	yes	yes	yes	**yes**	**yes**
Rinzel	yes	yes	yes	no	**no**	**yes**
lamprey halfcenter	yes	yes	yes	no	**no**	**yes**

5. A numerical example. To demonstrate the above results, we now analyze a pair of van der Pol oscillators in Lienard variables [28, Chap. XI], [29], with one-way excitatory coupling. At the end of the section simulation results of chains are also shown. The uncoupled units include a parameter p that can be varied to produce two characteristic behaviors. $p = 0$ corresponds to the classical van der Pol oscillator. Oscillator 1 is described by

$$\begin{aligned} \dot{x_1} &= f(x_1, y_1) = y_1, \\ \mu \dot{y_1} &= g(x_1, y_1) + \epsilon h(y_2) \end{aligned} \tag{5.1}$$

$$= \left(y_1 - y_1^3/3 - x_1\right) \cdot \left(1 + (p \cdot x_1)^4\right) + \epsilon \left\{ \begin{array}{lll} 1 & \text{if} & y_2 > 0 \\ 0 & \text{if} & y_2 \leq 0 \end{array} \right\}, \tag{5.2}$$

and the equations of oscillator 2 are the same but lack the coupling term $\epsilon\{\ldots\}$. The coupling obeys condition (i) and the uncoupled oscillators satisfy conditions (ii), (iii), and (iv) since $f_y \equiv 1$, the duty cycle is exactly 1/2 due to the symmetry of the vectorfield, and $f_x \equiv 0$. For $p = 0$, they also satisfy (v), because $g_x \equiv -1$. Thus they synchronize in the relaxation limit $\mu \to 0$ with extremely weak coupling (by Theorems 2.1 and 4.1) as well as with moderate coupling (by Theorems 3.1 and 4.1).

If $p \neq 0$, the S-shaped fast nullclines of (5.2) remain the same, but $g(x, y)$ becomes steeper as $|x_j|$ increases so that condition (v) does not hold and Theorem 4.1 cannot be applied. Numerical evaluations show that inequality (2.8) fails for $p < p_{cr} \approx 2.36$ but holds for $p \geq p_{cr}$. In the latter case, Theorems 2.1 and 3.1 predict persistent phase-shifts as $\mu \to 0$.

The oscillator pair was simulated with $\epsilon = 0.5$ and various values of μ and p. In every case, the system converged to a stable periodic orbit with period T equal to that of an uncoupled unit. The jth increasing zero-crossing of $y_1(t)$ and $y_2(t)$ (i.e., times t_{ij} when $y_i(t_{ij}) = 0$, $\dot{y}_i t_{ij} > 0$) were detected and the phase-shift Δ was determined according to

$$\Delta = \lim_{j \to \infty} \frac{t_{2j} - t_{1j}}{T}. \tag{5.3}$$

For weakly coupled relaxation oscillators ($\epsilon, \mu \to 0$), the respective meanings of $\pi > \Delta > 0$, $\Delta = 0$, and $-\pi < \Delta < 0$ are that the driven oscillator leads, is synchronous with, and lags behind the driver. Here ϵ is not very small, so $\Delta \approx 0$, but $\neq 0$ might also correspond

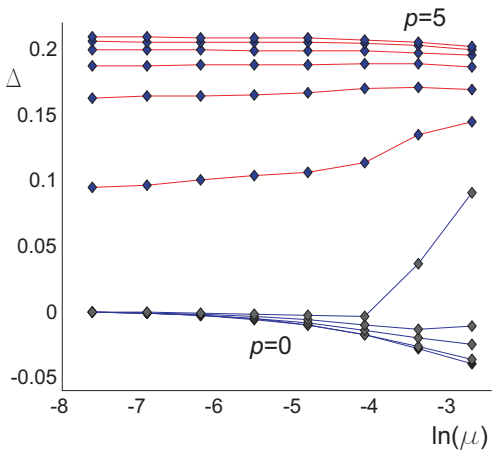

Figure 7. *Dependence of phase-shift between the coupled pair of oscillators* Δ *on* μ*. From bottom to top,* $p = 0, 0.5, 1, \ldots, 5$*. For small* p*, the shift is negative (the driven oscillator lags) and vanishes at the relaxation limit* $\mu \to 0$*; for large* p *the shift is positive and persists in the relaxation limit. Note that* $p = 2$ *is small in this regard, although it shows different behavior from the* $p < 2$ *cases for larger* μ *(fifth curve from the bottom).*

to synchrony (cf. the definition of synchrony in section 3.2). Nevertheless Δ is still a good indicator of the phase difference.

Figure 7 illustrates the dependence of Δ on μ for different values of p, showing that $\Delta(\mu)$ curves below 0, for small μ converge to 0 as $\mu \to 0$. Curves above 0, however, converge to a strictly positive limit. This corresponds to one of our main findings: if the driven oscillator leads the driver, the phase difference persists in the relaxation limit, but if the driver leads, the difference vanishes.

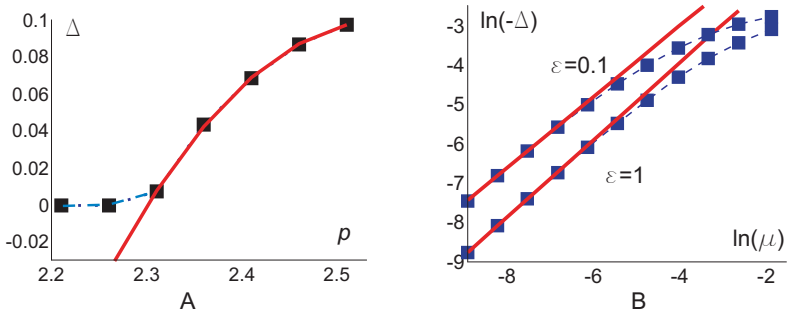

Figure 8. A: *Phase-shift* Δ *as function of* p *for* $\mu = 10^{-3}$*,* $\epsilon = 0.5$ *(squares), and a fitted quadratic curve* $\bar{\Delta}(p)$ *(solid line).* B: *Dependence of* Δ *on* μ *for* $p = 0$ *plotted on logarithmic scales for* $\epsilon = 1$ *and at* $\epsilon = 0.1$ *(squares). Linear regression in the range* $\mu = 10^{-4} \ldots 10^{-3}$ *reveals* $ln(-\Delta) \approx 0.98 \ln(\mu) + 0.04$ *and* $ln(-\Delta) \approx 0.90 \ln(\mu) + 0.67$*, respectively (solid lines).*

Figure 8(A) shows the numerically derived function $\Delta(p)$ for $\mu = 10^{-3}$ and $\epsilon = 0.5$. A quadratic fit for $\Delta > 0$ yields $\bar{\Delta}(p) = -1.646p^2 + 8.382p - 10.572$, whose root at $\bar{p}_{cr} \approx 2.301$ lies within 3% of $p_{cr} \approx 2.36$ predicted by inequality (2.8). The difference is primarily due to

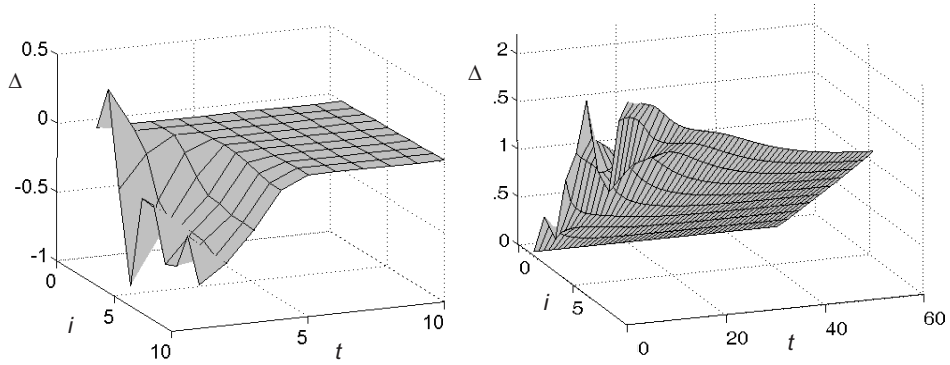

Figure 9. *Dynamics of a chain of* 10 *oscillators at* $p = 0$ *(left) and* 3 *(right). Each oscillator* i *is driven by its neighbor* $i-1$*;* t *denotes time normalized by the period of an uncoupled unit.* Δ *denotes the phase difference between units* i *and* 1*. Other parameter values:* $\epsilon = 0.5$*,* $\mu = 2 \cdot 10^{-3}$*.*

the relatively strong coupling.

We also determine numerically how Δ scales with μ for small p to examine $\lim_{\mu \to 0} \Delta = 0$. The predictions of sections 2.2 and 3.2 are $\Delta \backsim \mu^{2/3}$ for phase-oscillator interactions and $\Delta \backsim \mu^{1}$ for FTM interactions. According to simulations with $p = 0$, the exponent is approximately 0.97 in the range $\mu = 10^{-4} \ldots 10^{-3}$ if $\epsilon = 1$ and 0.90 if $\epsilon = 0.1$ (Figure 8(B)). These results reflect the fact that our parameter values are appropriate for FTM ($\mu << \epsilon << 1$); but they also show that the exponent decreases as ϵ decreases, moving toward the phase-approximation value, which holds for $\epsilon << \mu << 1$.

We close this section by illustrating the two types of behavior for chains. The two panels of Figure 9 show the spatio-temporal dynamics of phase-shifts along a chain of 10 unidirectionally coupled units. For $p = 0$ (left panel), the network rapidly synchronizes, while for $p = 3$ uniform phase-shifts develop on a longer time-scale. The final states agree with the predictions of Theorem 2.1. (The reason for the radically different decay times of transients is explained in [35].)

6. Applications to the lamprey CPG. The central pattern generator (CPG) of the lamprey has been a focus of research for over thirty years. Fictive swimming experiments [9] show that the CPG without muscles or afferent (feedback) inputs produces rhythms similar to real swimming: traveling waves of activation (motoneuron bursts) propagate from head to tail on both sides in antiphase. The wavelength remains approximately constant and equal to body length over a considerable speed range.

The components of the CPG and their interconnectivities have been partially determined [5], and a reduced network with three classes of neurons, representing one or a few segments of the animals' CPG, has been proposed; see Figure 10(A). Each segment has bilateral symmetry, with mutual inhibition between hemisegments. The entire CPG is modeled as a chain of such units [21, 23], intersegmental connections being of the same type as intrasegmental ones, but with strengths decreasing rapidly with distance. For simplicity here we assume only nearest-neighbor connections, but our results can be extended to more

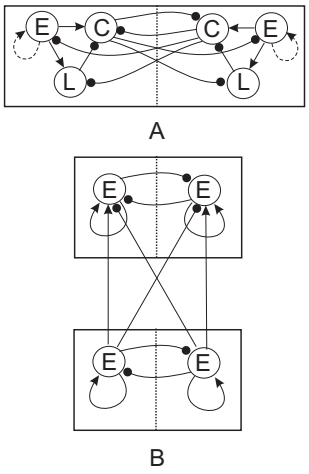

Figure 10. A: *Simplified structure of a segmental unit of the lamprey CPG first proposed by* [6]. *E, L, and C represent small groups of excitatory, crossed inhibitory, and lateral inhibitory neurons, respectively, and arrows and circles denote excitatory and inhibitory synapses. Bilaterally symmetric halves of the network are coupled by inhibition. The dashed self-excitatory connection occurs in some but not all models.* B: *A simplified network with E cells alone approximates the dynamics of cell-based rhythm generation (cf.* [38]*); two segmental units are shown.*

widespread connections, provided that they are short relative to the size of the full network.

Several models have implemented the network architecture of Figure 10(A), and two different pattern-generating mechanisms have been proposed [13]: rhythms being generated by network connections, or by small groups of bursting cells. Simple *network-based* models [4, 40] were able to reproduce the constant wavelength-swimming speed behavior, albeit over a limited frequency range. The *cell-based* mechanism inspired a series of detailed model studies [26, 39, 27] which encompass a wider frequency range, but with frequency-dependent wavelengths (small at low frequencies, large at high frequencies).

The core of the cell-based networks is a double chain of relaxation-type oscillators (Figure 10(B); see also [38]), each representing a small group of intrinsic bursters. The fast and the slow variables represent average activity (firing rate) and spike-rate adaptation due to slow calcium currents, respectively. In these models, swimming frequency is adjusted through serotonin concentration determining the speed of the slow dynamics, i.e., μ. (Other, less important, parameters also change with frequency, but we ignore these effects.) Thus, when swimming speed decreases, the speeds of the slow and the fast dynamics separate, approaching a relaxation limit. The tendency of chains of relaxation oscillators to synchronize offers a straightforward explanation for the wavelength-frequency behavior of these networks, and, as we now show, the results of sections 2–4 yield more precise predictions on cell-based CPG models.

The double chains of Figure 10 differ from the single chains studied in sections 2.3 and 3.3, but their behavior can be predicted in a similar manner by considering a pair of segments comprising four oscillators, as in Figure 10(B). Specifically, we assume condition (i) above, that the hemisegments remain out of phase, and we denote the strengths of intersegmental excitatory and inhibitory connections by ϵ_e and ϵ_i, respectively. Phase response theory

then yields the averaged coupling function $H_{\mu\,pair}$ governing intersegmental phase differences (cf. (2.4)) at given values of μ by superposing the contributions of the excitatory and inhibitory connections. In the relaxation limit $\lim_{\mu\to 0} H_{\mu\,pair} \stackrel{\text{def}}{=} H_{0\,pair}$ we obtain

$$\lim_{\mu\to 0} H_{\mu\,pair} \stackrel{\text{def}}{=} H_{0\,pair}(\psi) = \frac{1}{2\pi}\left[\epsilon_e \int_{\psi}^{D+\psi} z^*(\phi)\,d\phi - \epsilon_i \int_{\psi+\pi}^{D+\psi+\pi} z^*(\phi)\,d\phi\right]. \tag{6.1}$$

Equation (6.1) is the analogue of (2.7) with a second term $-\epsilon_i \int \ldots$ due to inhibition between the segments. Its consequence is a somewhat weaker and (in part (a)) more technical analogue of Theorem 2.1.

Theorem 6.1. *Let $(x, y) = (\xi, \upsilon(\xi))$ and $(x, y) = (\xi, \zeta(\xi))$, respectively, denote points on the active and silent branches of the $\dot{y} = 0$ nullcline. Assume that $\Delta(\mu)$ satisfies $dH_{\mu\,pair}(\psi)/d\psi|_{\Delta(\mu)} < 0 = H_{\mu\,pair}(\Delta(\mu))$.*

(a) *If conditions* (i)–(iii) *hold, and*

$$\begin{aligned} &-\epsilon_e \int_{x(0)}^{x(D)} \frac{f_y(\xi,\upsilon(\xi))}{f^2(\xi,\upsilon(\xi))g_y(\xi,\upsilon(\xi))}\,d\xi \\ &+\epsilon_i \int_{x(\pi)}^{x(\pi+D)} \frac{f_y(\xi,\zeta(\xi))}{f^2(\xi,\zeta(\xi))g_y(\xi,\zeta(\xi))}\,d\xi \\ &+\epsilon_e \frac{1}{g_x(x(D),y(D))}\left[\frac{1}{f(x(D),y(D))} - \frac{1}{f(x(D),y(D+))}\right] > 0, \end{aligned} \tag{6.2}$$

then for a coupling function of the form $H_{0\,pair}(\phi) = \Xi(\phi) + c$ (where Ξ is an arbitrary 2π periodic function and c is an arbitrary constant), there exists $\delta > 0$ independent of c such that if $|\Delta(0)| < \delta$, then $\Delta(0) > 0$.

(b) *If conditions* (i)–(iii) *hold, Δ is unique modulo 2π, and inequality* (6.2) *is false, then $\Delta(\mu) \backsim -\mu^{2/3}$ for small μ, and $\Delta(0) = 0$; i.e., the driven segment lags the driver and the segments synchronize in the relaxation limit.*

Proof (sketch). The proof of Theorem 6.1 is similar to that of Theorem 2.1, so we outline only the main points and differences between them.

Referring to (6.1) and the proof of Theorem 2.1, and noting that (6.2) has no "boundary" term due to inhibitory connections ϵ_i, since for duty cycle $D/(2\pi) < 0.5$ and $\phi_{ij} \approx 0$ the driven oscillator jumps when the inhibitory driver is inactive, we see that the left-hand side of inequality (6.2) is equal to $H_{0\,pair}(0)$. Hence, cases (a) and (b) of the theorem respectively correspond to $H_{0\,pair}(0) > 0$ and ≤ 0. The first term $\epsilon_e \int \ldots$ in (6.1) has a jump at $\phi = 0$, at the top of which it is positive, and this term is continuous on the left side of the jump provided that $-D < \phi < 0$ (see the proof of Theorem 2.1). The second term $-\epsilon_i \int \ldots$ is positive and continuous in ϕ if $|\phi| < (\pi - D)$ because z^* is negative and integrable in the interval $D < \phi < 2\pi$; cf. Figure 3. Hence, $H_{0\,pair}(\phi)$ itself has a jump at 0, is positive at the top of the jump ($H_{0\,pair}(0^-) > 0$), and is continuous in the interval $(-\min\{D, \pi - D\}, 0)$.

In case (b), at the bottom of the jump $H_{0\,pair}(0^+)$ is negative as in Theorem 2.1, so it has a stable root at 0, and because of uniqueness, $\Delta(0) = 0$. For μ small but positive, $\Delta(\mu) \backsim -\mu^{2/3}$ for the same reason as in Theorem 2.1. In case (a) at the bottom of the jump $H_{0\,pair}(0^+)$ is already positive, and thus $H_{0\,pair}(0^-) > s > 0$, where s denotes the magnitude

of the jump, which is independent of the constant c in the definition of $H_{0\,pair}$. On the negative side of 0, there is an interval in which $H_{0\,pair}(\phi)$ is continuous (see above). Thus by definition there exists δ (again independent of c) such that for arbitrary $0 < 0 - \phi < \delta$, we have $|H_{0\,pair}(0^-) - H_{0\,pair}(\phi)| < s$, yielding $H_{0\,pair}(\phi) > 0$. Thus if $|\Delta(0)| < \delta$, $\Delta(0)$ must be positive. ■

The implication of part (a) is that if $|\Delta(0)| << 1$, then $\Delta(0) > 0$; the driven segment leads the driver. Hence the statement in part (a) is similar to, and more specific than, part (a) of Theorem 2.1. Theorem 6.1 has two restrictions in addition to those of Theorem 2.1—the uniqueness of Δ in part (b) and its closeness to zero in part (a)—but neither affects its applicability to lamprey CPGs. Uniqueness means that the CPG has a unique stable traveling wave solution in agreement with the observation that the lamprey exhibits a single robust pattern of motion. It is also reasonable that $|\Delta(0)| << 1$ since the lamprey's notocord has $\mathcal{O}(100)$ segments, so intersegmental phase differences must be $\mathcal{O}(0.01 \times 2\pi)$ if wavelength is to equal body length.

Phase response theory does not always apply to the lamprey CPG, because intersegmental coupling is not necessarily weak, so FTM interactions may be more appropriate. Much as Theorem 2.1 has an analogous statement in Theorem 3.1, an analogue of Theorem 6.1 holds under the assumption of FTM interactions. Here we give an informative but inexact version, without proof.

Theorem 6.2. *Assume that two pairs of oscillators in the FTM limit ($\epsilon_{e,i} \to 0$, $\mu/\epsilon_{e,i} \to 0$) each have stable T-periodic solutions. Let Δ_{FTM} denote the time difference between activation of the ipsilateral driven and driver oscillators (positive if the driven activates first). Then,*

(a) *if conditions* (i)–(iii) *and inequality* (6.2) *hold and $|\Delta_{FTM}| << 1$, then the driven oscillators lead the drivers; and*

(b) *if conditions* (i)–(iii) *hold but inequality* (6.2) *fails and the network has only one stable T-periodic solution, then the oscillators synchronize (away from the relaxation limit, the driven segment lags the driver).*

Provided that the CPG has unidirectional intersegmental coupling, the consequences of Theorems 6.1–6.2 for the lamprey are as follows.

1. If inequality (6.2) fails, neighboring segments display a negative phase difference that vanishes in the relaxation limit. A chain will therefore exhibit waves that propagate in the direction of the intersegmental coupling, with wavelength approaching zero in the relaxation limit. Hence, in such models the wavelength is usually an increasing function of μ, instead of a constant with frequency. This behavior was seen in previous numerical simulations.

2. If inequality (6.2) holds, segments have positive phase differences that persist in the relaxation limit and traveling waves will propagate against the coupling direction, with approximately constant wavelength as μ is varied. Hence, intersegmental connections must be directed from tail to head to obtain head-to-tail traveling waves.

Our first important finding is that, if (6.2) holds, a double chain of oscillators can combine the advantages of previous cell- and network-based CPG models, namely, wide frequency-range and constant wavelengths. Theorem 4.1 implies that single chains rarely satisfy the analogous inequality (2.8), but the presence of an additional positive term $\epsilon_i \int \ldots$ in (6.2), due to cross-inhibitory connections, provides more flexibility. On the other hand, as shown in section 3.3, the bidirectional coupling in the real network promotes synchrony under the

assumption of FTM interactions. Hence finding "well-behaved" models is difficult, but probably not hopeless, since the high number of ad hoc parameters in such models allows wide freedom for improvement. The failure of such an attempt would suggest that the cell-based mechanism is an oversimplification and that more sophisticated models, perhaps combining both rhythm-generating mechanisms, are required.

It is also worth noting that caudo-rostral (tail-to-head) coupling is required to produce waves that travel from head to tail. This confirms previous studies [41, 20] that used completely different arguments to show that ascending is stronger than descending coupling in the lamprey notocord.

7. Conclusions. This paper concerns coupled sets of planar relaxation oscillators. We focus on pairs of oscillators with unidirectional coupling but draw conclusions for two-way coupling and linear chains of oscillators. Our main theorems, Theorems 2.1 and 3.1, provide sufficient conditions for persistent phase lags and for synchrony in the limits of weak coupling and of large time-scale separation, using phase response theory and FTM theory, respectively. The key step involves estimation of an inequality (2.8) arising from the averaged coupling function.

Theorem 4.1 provides a sufficient condition for synchrony, and in section 4 we show that several models of bursting neurons satisfy this condition, which we conjecture to be the typical case. However, counterexamples can be found, as demonstrated in section 5. Finally, in section 6 we extend these results to the double chains featured in models of CPGs for swimming in lamprey, providing analogues of Theorems 2.1 and 3.1 in Theorems 6.1 and 6.2. These results partially explain why cell-based models of relaxation type approach synchrony as swimming speed decreases, violating the experimental observation of near-constant phase lags over a wide speed range, but they also offer hope that parameterizations that permit the observed behavior may be found.

More generally, the results in this paper reveal interesting relations between phase response and FTM theory, which apply in the distinctly different limits of weak coupling ($1 \gg \mu \gg \epsilon \to 0$) and strong time-scale separation ($1 \gg \epsilon \gg \mu \to 0$). In particular, we construct a composed Poincaré return map in the latter relaxation limit that is the analogue of the averaged coupling function in the former limit. This map is used to demonstrate that the tendency of unidirectionally coupled pairs or arrays of oscillators to synchronize is unaffected by extreme changes of the ratio ϵ/μ despite evident differences between the resultant coupling mechanisms. However, we also find that the rates of convergence to synchrony scale differently as perfect time-scale separation ($\mu \to 0$) is approached. In case of FTM interaction, our study raises further questions regarding the behavior of bidirectionally but asymmetrically coupled arrays as well as that of arrays with multiple (non–nearest-neighbor) coupling. A similar approach to the present one may be helpful in studying synchronization properties of such networks.

Appendix A. Theorem 2.1: The PRC at jumps. Here we locally approximate the PRC near jumps, showing that relaxation oscillators have large phase response values during transition, shortly before (but not during) jumps. This fact is central in the proof of Theorem 2.1.

We assume small but nonzero μ, in which case the stable limit cycle Γ of the ODEs (2.1)–(2.2) is close to but not exactly the same as that shown in Figure 1. Since notation like $x(\phi)$

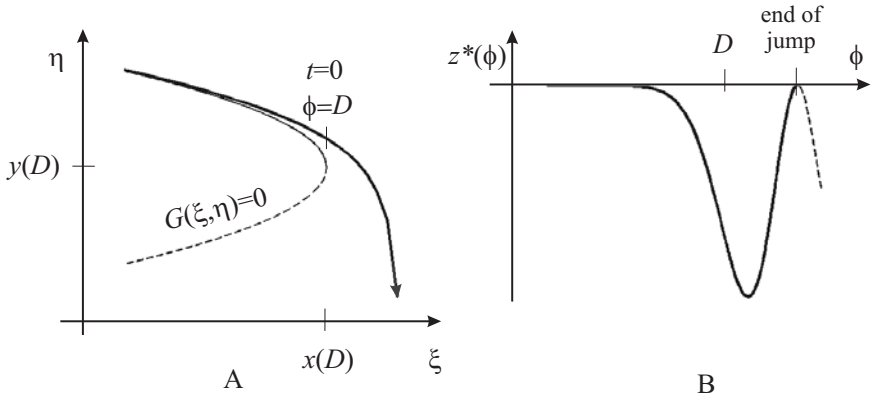

Figure 11. A: *An orbit in the neighborhood of a downward jump.* B: *The PRC near the jump.*

has been used to denote coordinates on Γ as $\mu \to 0$, we now use different notation ξ and η for the slow and the fast variables, respectively. We define time t and phase ϕ such that $t = 0$ and $\phi = D$ when $\xi = x(D)$; see Figure 11(A).

Leading order terms in the PRC near jumps at nondegenerate (quadratic) turning points are determined by the local approximation

$$\dot{x} \approx f(x(D), y(D)), \tag{A.1}$$

$$\mu\dot{y} \approx g_x(x(D), y(D))\,[x - x(D)] + \frac{g_{yy}(x(D), y(D))}{2}\,[y - y(D)]^2\,. \tag{A.2}$$

These ODEs have an explicit solution in terms of Airy functions and their derivatives [1], denoted below by Ai, Bi, Ai', and Bi':

$$\xi(t) = x(D) + ft, \tag{A.3}$$

$$\eta(\xi) = y(D) + \mu^{1/3}\left(\frac{4fg_x}{g_{yy}^2}\right)^{1/3}\frac{Ai'(\zeta) + a \cdot Bi'(\zeta)}{Ai(\zeta) + a \cdot Bi(\zeta)}, \tag{A.4}$$

where a is an arbitrary constant, the arguments $(x(D), y(D))$ have been suppressed (i.e., $f = f(x(D), y(D))$, etc.), and ζ is a rescaled version of ξ,

$$\zeta = -\mu^{-2/3}\left(\frac{g_x g_{yy}}{2f^2}\right)^{1/3}(\xi - x(D)). \tag{A.5}$$

The parameter a is determined by the asymptotic boundary condition that for $\xi \to -\infty$ the orbit follows the upper branch of the $g = 0$ nullcline, implying that $\eta(\xi) > y(D)$; see Figure 11(A). We note that $\xi \to -\infty$ corresponds to $\zeta \to \infty$ by (A.5), the limiting values of $Ai(\zeta)$, $Ai'(\zeta)$, $Bi(\zeta)$, and $Bi'(\zeta)$ are $+0$, -0, $+\infty$, and $+\infty$, respectively, and, from the nullcline geometry, $f > 0 > g_x$. Using these facts in (A.4), $\lim_{\xi\to-\infty}\eta(\xi) > y(D)$ implies that $a = 0$. The orbit gradually leaves the nullcline and η goes to minus infinity at $\zeta = A \approx -2.3381$, which is a zero of the function Ai. The term $\mu^{1/3}$ in (A.4) implies that, for small μ, η remains close to zero for most values of ζ and suddenly grows just before ζ reaches its critical value.

By definition, the PRC represents the (linear) advancing or retarding effect of a small, instantaneous perturbation $\Delta\eta$ in the fast variable. Such a perturbation results in a switch to another trajectory with $a \approx \Delta\eta \cdot da/d\eta$. The η-coordinate of the perturbed trajectory goes to infinity at $\zeta = \zeta_{end}(a)$. We assume that $\zeta_{end}(a)$ corresponds, via (A.5), to the rescaled slow coordinate ξ_{end} when the jump is finished and slow motion begins on the lower branch of the nullcline; as already noted, $\zeta_{end}(0) = A$. The perturbation changes this by

$$\Delta\xi_{end} = \Delta\eta \frac{da}{d\eta}\frac{d\zeta_{end}}{da}\frac{d\xi}{d\zeta} + \mathcal{O}(\Delta\eta^2). \tag{A.6}$$

To compute the effect of the perturbation, note that during the jump the slow variable evolves according to $\dot{\xi} \approx f(x(D), y(D))$, so that the jump duration increases by $\Delta\xi_{end}/f(x(D), y(D))$. After the jump, the orbit reverses direction in ξ: $\dot{\xi} \approx f(x(D), y(D^+)) < 0$. Thus positive $\Delta\xi$ has a further retarding effect of duration $\Delta\xi_{end}/f(x(D), y(D^+))$. The sum of these two terms represents the "time-response" to the perturbation, and a final scaling factor $d\phi/dt = \omega$ yields the local PRC

$$\begin{aligned}\Delta\phi = -\Delta\eta \frac{da}{d\eta}\frac{d\zeta_{end}}{da}\frac{d\xi}{d\zeta}\omega \left[f^{-1}(x(D), y(D)) - f^{-1}(x(D), y(D^+))\right] \\ + \mathcal{O}(\Delta\mu^2),\end{aligned} \tag{A.7}$$

where the minus sign implies that positive values correspond to shortening of the period.

We compute the components of the product in (A.7) one by one. First, $d\xi/d\zeta$ comes directly from (A.5):

$$\frac{d\xi}{d\zeta} = -\mu^{2/3}\left(\frac{2f^2}{g_x g_{yy}}\right)^{1/3}. \tag{A.8}$$

We find $da/d\eta = (d\eta/da)^{-1}$ using (A.4):

$$\begin{aligned}\frac{da}{d\eta} &= \left[\left(\frac{4\mu f g_x}{g_{yy}^2}\right)^{1/3} \frac{Bi'(\zeta)(Ai(\zeta) + a\,Bi(\zeta)) - Bi(\zeta)(Ai'(\zeta) + a\,Bi'(\zeta))}{(Ai(\zeta) + a\,Bi(\zeta))^2}\bigg|_{a=0}\right]^{-1} \\ &= \left[\left(\frac{4\mu f g_x}{g_{yy}^2}\right)^{1/3} \frac{Bi'(\zeta)\,Ai(\zeta) - Bi(\zeta)\,Ai'(\zeta)}{Ai(\zeta)^2}\right]^{-1}.\end{aligned} \tag{A.9}$$

The term $Bi'(\zeta)\,Ai(\zeta) - Bi(\zeta)\,Ai'(\zeta)$ is constant. The fact that its derivative is 0 follows from the definition of Airy functions: $v\,Ai(v) = Ai''(v)$, $v\,Bi(v) = Bi''(v)$. This straightforward calculation is omitted. Hence we may replace ζ by the constant $A \approx -2.3381$ defined above and use $Ai(A) = 0$ to obtain

$$\frac{da}{d\eta} = -\left[\left(\frac{4\mu f g_x}{g_{yy}^2}\right)^{1/3} \frac{Bi(A)\,Ai'(A)}{Ai(\zeta)^2}\right]^{-1}. \tag{A.10}$$

Finally, we determine $d\zeta_{end}/da$. $\zeta_{end}(a)$ denotes the location of the singularity in (A.4): it is the solution of

$$Ai(\zeta) + a\,Bi(\zeta) = 0. \tag{A.11}$$

Thus we have

$$\frac{d\zeta_{end}}{da} = \left[\frac{da}{d\zeta_{end}}\right]^{-1} = \left[-\frac{d\left[Ai(\zeta)/Bi(\zeta)\right]}{d\zeta}\bigg|_{\zeta=A}\right]^{-1}$$
$$= \frac{Bi^2(A)}{Ai(A)\,Bi'(A) - Ai'(A)\,Bi(A)} = -\frac{Bi(A)}{Ai'(A)}. \tag{A.12}$$

Substituting (A.3), (A.5), (A.8), (A.10), and (A.12) into (A.7), we obtain the PRC in terms of t:

$$\frac{\Delta\phi}{\Delta\eta} \approx \left[\frac{\mu f(x(D),y(D))g_{yy}(x(D),y(D))}{2g_x^2(x(D),y(D))}\right]^{1/3} Ai'^{-2}(A)$$
$$\times\, Ai^2\left(-\mu^{-2/3}\left(\frac{g_x(x(D),y(D))g_{yy}(x(D),y(D))f(x(D),y(D))}{2}\right)^{1/3} t\right)$$
$$\times\, \omega\left[\frac{1}{f(x(D),y(D))} - \frac{1}{f(x(D),y(D^+))}\right]. \tag{A.13}$$

Finally, replacing t by $\phi = \phi_0 + \omega t$, we obtain the approximate PRC $z(\phi)$ during the transition and jump. Note that in spite of its apparent complexity, the formula (A.13) contains only constants and a scaled Ai^2 function, so that we may write

$$z^*(\phi) = \frac{z(\phi)}{\mu} \approx B\mu^{-2/3}\, Ai^2\left(C\mu^{-2/3}(\phi - \phi_0)\right), \tag{A.14}$$

where B, C are $O(1)$ constants. See also Figure 11(B).

This formula demonstrates that large PRC values occur during transition, while the oscillator state is near the upper nullcline. (These correspond to the delta function in the relaxation limit; see (2.6).) The analogous result for the upward jump can be derived in the same way. In that case, the large values occur during transition at the lower nullcline. We remark, without explicit computations, that the integral of this approximation of the phase-response function from $-\infty$ to the end of the jump is equal to the coefficient of the delta function in (2.6).

Appendix B. Proof of Theorem 3.1. The proof is divided into five parts. In the first, notation and concepts are introduced; these include four mappings H_i representing the interactions of the oscillators during the four segments of their limit cycles (slow motions on the upper and lower nullcline branches, and jumps). In the second part we analyze the functions H_i. These results are used in the third part to demonstrate that the only possible forms of T-periodic interactions are synchrony or O_1 leading O_2. The fourth part contains the proof that if O_1 leads, then inequality (2.8) holds, and in the last part we show the converse in the case of synchrony.

B.1. Notation. Let $t_j^{(1)}, \ldots, t_j^{(5)}$ denote the times at which the state of O_j successively crosses the Poincaré sections $\Pi_1, \Pi_2, \ldots, \Pi_5 = \Pi_1$ defined in Figure 6(A). We shall construct a return map

$$\epsilon H_{FTM}(t_2^{(1)} - t_1^{(1)}) = \left[t_2^{(5)} - t_1^{(5)}\right] - \left[t_2^{(1)} - t_1^{(1)}\right], \tag{B.1}$$

which describes the time-shift during one cycle due to coupling, normalized by the coupling strength ϵ. Phase-locked solutions correspond to zeros of H_{FTM}, and their stability requires $0 \le \epsilon\, dH_{FTM}(t)/dt \le 2$. Thus, H_{FTM} is a similar predictor of dynamics to the coupling function $H(\psi)$ in the phase limit, although the stability condition differs. We assemble the maps H_i, $i = 1, 2, 3, 4$,

$$\epsilon H_i(t_2^{(i)} - t_1^{(i)}) = \left[t_2^{(i+1)} - t_1^{(i+1)}\right] - \left[t_2^{(i)} - t_1^{(i)}\right], \tag{B.2}$$

the composition of which defines

$$\begin{aligned} H_{FTM}(t) = {} & H_1(t) + H_2(t + \epsilon H_1(t)) \\ & + H_3(t + \epsilon H_2(t + \epsilon H_1(t))) \\ & + H_4(t + \epsilon H_3(t + \epsilon H_2(t + \epsilon H_1(t)))). \end{aligned} \tag{B.3}$$

In Figure 6(A), we introduce notation for the times required to travel along certain trajectories in the phase space. We use these to express the functions H_i for small ϵ in the next subsection. The notation reflects the scaling of these lengths; e.g., $\epsilon\Delta\tau_2$ in Figure 6(A) is $\mathcal{O}(\epsilon)$ because it represents the effect of a perturbation of strength $\mathcal{O}(\epsilon)$ and duration $\mathcal{O}(1)$.

B.2. The functions H_i. We shall use condition (iii), which implies that $\tau_4 > \tau_2$ if ϵ is sufficiently small. We also note that the functions H_i are invariant under translation by the period of the unperturbed limit cycle: $T = \epsilon(\tau_1 + \tau_1') + \tau_2 + \tau_4$.

To construct $H_1(t)$ we exploit the nature of FTM interactions. For $\epsilon\tau_1' \le t \le \tau_4$, O_1 receives no input between Π_1 and Π_2, so it travels on its unperturbed limit cycle, yielding $H_1(t) \equiv 0$. At $t = 0$, $H_1(0) = \epsilon\Delta\tau_1'$. If $-\epsilon\tau_1 - \tau_2 \le t \le -\epsilon\tau_1$, O_1 follows the perturbed limit cycle, so $H_1(t) \equiv (\tau_1 + \tau_1')$. For $-\epsilon\tau_1 \le t \le 0$, O_1 switches to the perturbed limit cycle from the curve of length $\epsilon\tau_1$, as shown in Figure 6(B). On the intervals $(-\epsilon\tau_1, 0)$ and $(0, \epsilon\tau_1')$, $H_1(t)$ is approximately linear (for $\epsilon \ll 1$). See Figure 12(A). The mapping $H_3(t)$ is generated in much the same way (Figure 12(C)).

To approximate $H_2(t)$ we use condition (ii), which implies that orbits move faster on the upper branch of the perturbed nullcline than on the unperturbed one: $\Delta\tau_2$ is positive. Thus for $t = 0$, O_1 receives input along the upper nullcline and arrives at Π_3 before O_2, so $H_2(0) = \Delta\tau_2$. The same argument holds if t is slightly negative, but if t is further decreased, the coupling signal turns off before O_1 reaches Π_3, until at $t = -\tau_2$ O_1 reaches Π_3 entirely on the unperturbed limit cycle. Thus $H_2(t) \equiv 0$ for $t < -\tau_2$, and it increases monotonically for $-\tau_2 < t$. See Figure 12(B).

O_1 receives input while traveling between Π_2 and Π_3, if $t \in (0, \epsilon\tau_1')$, so $H_2(t) \equiv \Delta\tau_2$ in this interval. If, however, t is increased further, O_1 has no input when crossing Π_2, and it first follows the unperturbed nullcline and jumps to the perturbed one if $t \in (\epsilon\tau_1', \epsilon\tau_1' + \tau_2)$; the bigger t is, the later this jump occurs. Thus H_2 decreases in this interval. If $t > \epsilon\tau_1' + \tau_2$, again $H_2(t) \equiv 0$.

Similar arguments lead to $H_4(t)$ (Figure 12(D)). $H_4(t) \equiv 0$ for $t \in (-\epsilon\tau_1, 0)$, because O_1 travels on the unperturbed nullcline. Because of condition (ii), traveling on the perturbed nullcline is always slower; thus $H_4(t)$ is nonpositive. It is monotonically decreasing in $(0, \tau_2 + \epsilon\tau_1')$, at which point O_1 starts on the perturbed limit cycle but switches along the

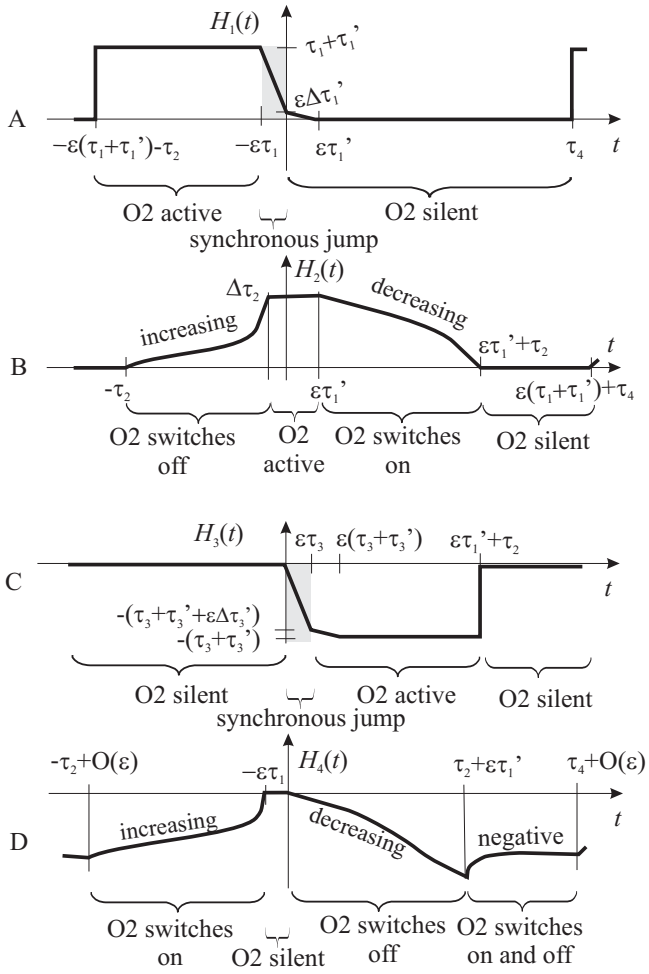

Figure 12. *The maps H_i.* A: O_2 active/silent *implies that O_2 is active/silent when O_1 jumps up;* synchronous jump *means that the upward jump of O_2 initiates an immediate jump in O_1.* B: O_2 active/silent *applies for the time interval in which O_1 travels from Π_2 to Π_3; O_2* switches on/off *means that O_2 is silent/active when O_1 crosses Π_2 but switches on/off before O_1 reaches Π_3. Analogous notation is used in* C *and* D.

way. The bigger t is, the longer it travels before switching to the unperturbed nullcline. H_4 has another, increasing part, corresponding to traveling on the unperturbed nullcline initially and switching to the perturbed one at some point (the bigger t, the later this happens), and a fourth region, marked "negative" in Figure 12(D), corresponding to starting and arriving on the unperturbed nullcline and spending an interval of length $\tau_2 + \epsilon\tau_1'$ on the other nullcline in between.

B.3. Possible forms of T-periodic dynamics. Here we show that on any stable T-periodic solution of the coupled oscillator pair, either O_1 and O_2 are in synchrony or O_1 leads O_2. We thereby exclude alternating dynamics or leading by O_2.

First assume that the oscillators alternate, so that, while O_2 is active, O_1 moves between Π_3 and Π_4. Thus, $t + \epsilon H_3(t + \epsilon H_2(t + \epsilon H_1(t))) \in (\tau_2 + O(\epsilon), \tau_4 + O(\epsilon))$: the interval marked

negative in Figure 12(D). This implies that

$$t \in (\tau_2 + O(\epsilon),\, \tau_4 + O(\epsilon)), \tag{B.4}$$

and while (B.4) holds, we can deduce the following.

1. From (B.4) and the fact that O_2 is silent when O_1 jumps up, $H_1(t) \equiv 0$ for sufficiently small ϵ.
2. Because O_2 is silent when O_1 is on its upper nullcline, $H_2(t + \epsilon H_1(t)) \equiv 0$.
3. Because O_2 is silent when O_1 jumps down, $H_3(t + \epsilon H_2(t + \epsilon H_1(t))) \equiv 0$.
4. From (B.4), $H_4(t + \epsilon H_3(t + \epsilon H_2(t + \epsilon H_1(t)))) < 0$.

Thus, $H_{FTM} < 0$ by (B.3). Since T-periodic solutions require $H_{FTM}(t) = 0$, this is a contradiction.

Assume now that O_2 leads O_1. In this case, the following hold:

1. O_2 is active when O_1 jumps up, corresponding to the $H_1(t) = \text{const} > 0$ part of H_1.
2. O_2 turns off before O_1 reaches Π_3, corresponding to the increasing part of H_2.
3. O_2 is silent when O_1 is between Π_3 and Π_4, implying that $H_3(t+\epsilon H_2(t+\epsilon H_1(t))) \equiv 0$.
4. O_2 turns on before O_1 reaches Π_1, corresponding to the increasing part of H_4.

In the interval of t that satisfies these requirements, all four functions are constant or increasing, implying that $H_{FTM}(t)$ itself is constant or increasing and hence that T-periodic solutions, if any exist, are unstable, from section B.1. This is again a contradiction.

Thus, we have proven that the only possible stable T-periodic solutions are synchrony or leading of O_1. In the next two subsections, we show that, if ϵ is sufficiently small, inequality (2.8) determines which case occurs.

B.4. If O_1 leads, then inequality (2.8) holds. Assume now that $H_{FTM}(t) = 0$ and O_1 leads. In this case O_2 is silent when O_1 is between Π_1 and Π_2, so that $H_1(t) < \epsilon\,\Delta\tau_1'$; see Figure 12(A). Similarly, O_2 is active when O_1 lies between Π_3 and Π_4, implying that $H_3(t + \epsilon H_2(t + \epsilon H_1(t))) < -(\tau_3 + \tau_3') + \epsilon\Delta\tau_3'$; see Figure 12(C). Combining these with the global inequalities $H_2 \le \Delta\tau_2$ and $H_4 \le 0$, (B.3) yields

$$0 = H_{FTM}(t) < \epsilon\Delta\tau_1' - (\tau_3 + \tau_3') + \epsilon\Delta\tau_3' + \Delta\tau_2. \tag{B.5}$$

The $\mathcal{O}(\epsilon)$ terms vanish as $\epsilon \to 0$; limiting values of the $\mathcal{O}(1)$ terms are found below.

For $\epsilon \ll 1$ (weak coupling) $\epsilon\Delta\tau_2$ is equal to the (appropriately scaled) linear phase-response to continuous ϵ perturbation during slow motion on the upper branch ($0 < \phi < D$); i.e., as shown in section 2,

$$\lim_{\epsilon\to 0} \Delta\tau_2 = \int_{x(0)}^{x(D)} \frac{f_y(\chi, y_a(\chi))}{f^2(\chi, y_a(\chi)) g_y(\chi, y_a(\chi))}\, d\chi. \tag{B.6}$$

We obtain $(\tau_3 + \tau_3')$ in the $\epsilon \to 0$ limit by approximating the ODEs defining O_1 at the upper right knee $[x(D), y(D)]$ by (A.1)–(A.2), derived in Appendix A. Substituting $h = 1$ and solving

$$g(x, y) + \epsilon \cdot 1 = 0 \quad \text{and} \quad g_y(x, y) = 0 \tag{B.7}$$

shows that the perturbation ϵh shifts the knee to the right by $\epsilon/g_x(x(D), y(D))$. Thus,

$$\epsilon\tau_3 \approx -\frac{\epsilon}{f(x(D), y(D))g_x(x(D), y(D))}, \tag{B.8}$$

$$\text{and} \quad \epsilon\tau_3' \approx \frac{\epsilon}{f(x(D), y(D^+))g_x(x(D), y(D))}, \tag{B.9}$$

yielding

$$\tau_3 + \tau_3' \approx \frac{1}{g_x(x(D), y(D))}\left[\frac{1}{f(x(D), y(D))} - \frac{1}{f(x(D), y(D^+))}\right]. \tag{B.10}$$

Substituting (B.6) and (B.10) into (B.5), we find that (2.8) holds in the $\epsilon \to 0$ limit. ■

Note that (B.10) represents the effect of FTM interactions but that it also agrees with predictions of phase reduction theory; cf. (2.6). This is the main reason that condition (2.6) holds in both the phase and the FTM limits.

B.5. Inequality (2.8) is false in case of synchrony. First we substitute the inequalities $H_1 \geq 0$ and $H_3 \geq -(\tau_3 + \tau_3')$ (cf. Figures 12(A,C)) into (B.3) to obtain

$$0 = H_{FTM}(t) \geq H_2(t + \epsilon H_1(t)) - (\tau_3 + \tau_3') + H_4(t + \epsilon H_3(t + \epsilon H_2(t + \epsilon H_1(t)))). \tag{B.11}$$

$H_2(t + H_1(t))$ is estimated by noting that, in case of synchrony, at least one of the following holds:

1. Upward jumps are synchronous.
2. Downward jumps are synchronous.
3. O_1 jumps up earlier and jumps down later than O_2.
4. O_2 jumps up earlier and jumps down later than O_1.

The first case yields $|t| \leq \epsilon\tau_1$; cf. Figure 12(A). Since $|H_1| \leq \tau_1 + \tau_1'$, we also have $|t + \epsilon H_1(t)| \leq \epsilon(\tau_1 + 2\tau_1')$; i.e., for arbitrary $\delta_1 > 0$, sufficiently small ϵ guarantees $|t + \epsilon H_1(t)| \leq \delta_1$. In the limit $\epsilon \to 0$, H_2 is determined exactly by phase theory. Moreover, H_2 is continuous because it describes interactions that occur only during slow dynamics and not during jumps. Appealing to continuity, we see that for arbitrary $\delta_2 > 0$, we may pick δ_1 sufficiently small that $|H_2(v) - H_2(0)| \leq \delta_2$ for all $|v| \leq \delta_1$. Thus, for ϵ sufficiently small, we conclude that

$$H_2(t + \epsilon H_1(t)) \geq \Delta\tau_2 - \delta_2. \tag{B.12}$$

Analogous arguments can be applied in the other three cases, and one can show in the same way that for sufficiently small ϵ, $|H_4(t + \epsilon H_3(t + \epsilon H_2(t + \epsilon H_1(t)))) - H_4(0)| \leq \delta_2$ also holds, implying that

$$H_4(t + \epsilon H_3(t + \epsilon H_2(t + \epsilon H_1(t)))) \geq -\delta_2. \tag{B.13}$$

Substituting inequalities (B.12)–(B.13) into (B.11), we obtain

$$0 = H_{FTM}(t) \geq \Delta\tau_2 - (\tau_3 + \tau_3') - 2\delta_2, \tag{B.14}$$

which holds for arbitrarily small δ_2 and so yields

$$0 \geq \Delta\tau_2 - (\tau_3 + \tau_3'). \tag{B.15}$$

Finally, using (B.6) and (B.10) in (B.15), we conclude that (2.8) cannot hold. ■

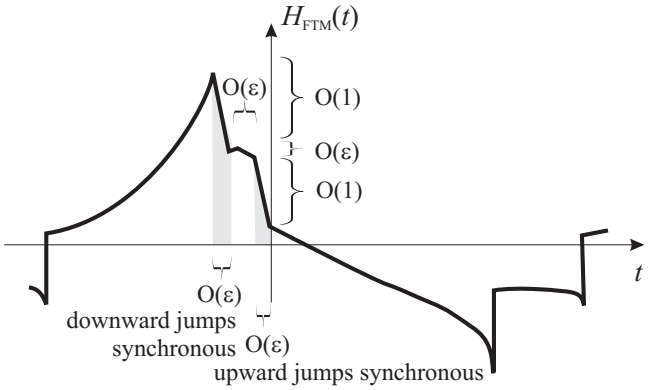

Figure 13. *An example of the composed map H_{FTM}. The proof of Theorem 3.1 relies on the fact that for $\epsilon \to 0$, the shape of H_{FTM} is similar to that of H in Figure 3. H_{FTM} has one or two steep, decreasing steps (two are shown here), inherited from H_1 and H_3. If there are two, they are separated by a plateau of width $O(\epsilon)$. A root of H_{FTM} in either steep part means that at least one jump is synchronous; a root in the plateau corresponds to synchronous activity in which neither jump is synchronous (cf. section 3.2). The latter is atypical in the limit $\epsilon \to 0$, as shown in Appendix C.*

Appendix C. Synchrony under weak coupling. The mappings H_2 and H_4 introduced in Appendix B have finite steepness, but H_1 and H_3 have $O(\epsilon^{-1})$-steep decreasing steps, corresponding to synchronous jumps of the two oscillators. The exact shape of the mapping H_{FTM} is model-specific, but in all cases it will also have one or two inherent steep parts due to (B.3), as shown in the example of Figure 13. According to the definition of section 3.2, the T-periodic orbits of the two oscillators are synchronous if one or both jumps coincide, or if one oscillator jumps up earlier but jumps down later than the other. These cases respectively correspond to two steep segments of H_{FTM} and the small plateau between them (if such a plateau exists). The width and height of the plateau is $O(\epsilon)$, and it vanishes in the limit $\epsilon \to 0$. Thus, synchronous activity typically means that either upward or downward jumps are synchronous.

REFERENCES

[1] M. Abramowitz and I. A. Stegun, eds., *Handbook of Mathematical Functions with Formulas, Graphs, and Mathematical Tables*, Wiley Interscience, New York, 1984.

[2] C. M. Bender and S. A. Orszag, *Advanced Mathematical Methods for Scientists and Engineers*, McGraw Hill, New York, 1978.

[3] E. Brown, J. Moehlis, and P. Holmes, *On the phase reduction and response dynamics of neural oscillator populations*, Neural Comp., 16 (2004), pp. 673–715.

[4] J. T. Buchanan, *Neural network simulations of coupled locomotor oscillators in the lamprey spinal cord*, Biol. Cybernet., 66 (1992), pp. 367–374.

[5] J. T. Buchanan, *Contributions of identifiable neurons and neuron classes to lamprey vertebrate neurobiology*, Progress in Neurobiol., 63 (2001), pp. 441–466.

[6] J. T. Buchanan and S. Grillner, *Newly identified glutamate interneurons and their role in locomotion in the lamprey spinal cord*, Science, 236 (1987), pp. 312–314.

[7] A. H. Cohen, P. J. Holmes, and R. H. Rand, *The nature of the coupling between segmental oscillators of the lamprey spinal generator for locomotion: A mathematical model*, J. Math. Biol., 13 (1982), pp. 345–369.

[8] A. H. Cohen, S. Rossignol, and S. Grillner, eds., *Neural Control of Rhythmic Movements in Vertebrates*, Wiley, New York, 1988.
[9] A. H. Cohen and P. Wallén, *The neuronal correlate of locomotion in fish. "Fictive swimming" induced in an in vitro preparation of the lamprey*, Exp. Brain Res., 41 (1980), pp. 11–18.
[10] S. Coombes, *Phase locking in networks of synaptically coupled McKean relaxation oscillators*, Phys. D, 160 (2001), pp. 173–188.
[11] G. B. Ermentrout and N. Kopell, *Multiple pulse interactions and averaging in systems of coupled neural oscillators*, J. Math. Biol., 29 (1991), pp. 195–217.
[12] R. FitzHugh, *Impulses and physiological states in models of nerve membrane*, Biophys. J., 1 (1961), pp. 445–466.
[13] S. Grillner, J. T. Buchanan, and A. Lansner, *Simulation of the segmental burst generating network for locomotion in lamprey*, Neuroscience Letters, 89 (1988), pp. 31–35.
[14] J. Guckenheimer, *Isochrons and phaseless sets*, J. Math. Biol., 1 (1975), pp. 259–273.
[15] J. Guckenheimer and P. J. Holmes, *Nonlinear Oscillations, Dynamical Systems and Bifurcations of Vector Fields*, Springer-Verlag, New York, 1983.
[16] J. L. Hindmarsh and R. M. Rose, *A model of the nerve impulse using two first-order differential equations*, Nature, 296 (1982), pp. 162–164.
[17] P. Holmes, R. J. Full, D. Koditschek, and J. Guckenheimer, *The dynamics of legged locomotion: Models, analyses, and challenges*, SIAM Rev., 48 (2006), pp. 207–304.
[18] F. C. Hoppensteadt and E. M. Izhikevich, *Weakly Connected Neural Networks*, Springer-Verlag, New York, 1997.
[19] E. M. Izhikevich, *Phase equations for relaxation oscillators*, SIAM J. Appl. Math., 60 (2000), pp. 1789–1804.
[20] T. Kiemel, K. M. Gormley, L. Guan, T. L. Williams, and A. H. Cohen, *Estimating the strength and direction of functional coupling in the lamprey spinal cord*, J. Comput. Neurosci., 15 (2003), pp. 233–245.
[21] N. Kopell, *Toward a theory of modelling central pattern generators*, in Neural Control of Rhythmic Movements in Vertebrates, A. H. Cohen, S. Rossignol, and S. Grillner, eds., Wiley, New York, 1988, pp. 369–413.
[22] N. Kopell and G. B. Ermentrout, *Symmetry and phaselocking in chains of weakly coupled oscillators*, Comm. Pure Appl. Math., 39 (1986), pp. 623–660.
[23] N. Kopell and G. B. Ermentrout, *Chains of oscillators in motor and sensory systems*, in The Handbook of Brain Theory and Neural Networks, 2nd ed., M. A. Arbib, ed., MIT Press, Cambridge, MA, 2003, pp. 201–205.
[24] N. Kopell and D. Somers, *Anti-phase solutions in relaxation oscillators coupled through excitatory interactions*, J. Math. Biol., 33 (1995), pp. 261–280.
[25] N. Kopell, W. Zhang, and G. B. Ermentrout, *Multiple coupling in chains of oscillators*, SIAM J. Math. Anal., 21 (1990), pp. 935–953.
[26] J. H. Kotaleski, A. Lansner, and S. Grillner, *Neural mechanisms potentially contributing to the intersegmental phase lag in lamprey* ii. *Hemisegmental oscillations produced by mutually coupled excitatory neurons*, Biol. Cybernet., 81 (1999), pp. 299–315.
[27] A. Lansner, O. Ekeberg, and S. Grillner, *Realistic modeling of burst generation and swimming in the lamprey*, in Neurons, Networks, and Motor Behavior, P. S. G. Stein, S. Grillner, A. I. Selverston, and D. G. Stuart, eds., MIT Press, Cambridge, MA, 1997, pp. 165–171.
[28] S. Lefschetz, *Differential Equations: Geometric Theory*, 2nd ed., Interscience Publishers, New York, 1963.
[29] A. Liénard, *Étude des oscillations entretenues*, Revue Générale de l'Électricité, 23 (1928), pp. 901–912, 946–954.
[30] I. G. Malkin, *Methods of Poincaré and Linstedt in the Theory of Nonlinear Oscillations*, Gostexisdat, Moscow, 1949 (in Russian).
[31] I. G. Malkin, *Some Problems in Nonlinear Oscillation Theory*, Gostexisdat, Moscow, 1956 (in Russian).
[32] C. Morris and H. Lecar, *Voltage oscillations in the barnacle giant muscle fiber*, Biophys. J., 35 (1981), pp. 193–213.
[33] J. S. Nagumo, S. Arimoto, and S. Yoshizawa, *An active pulse transmission line simulating a nerve axon*, Proc. IRE, 50 (1962), pp. 2061–2070.

[34] J. Rinzel, *Excitation dynamics: Insights from simplified membrane models*, Federation Proc., 44 (1985), pp. 2944–2946.
[35] D. Somers and N. Kopell, *Rapid synchronization through fast threshold modulation*, Biol. Cybernet., 68 (1993), pp. 393–407.
[36] D. Somers and N. Kopell, *Waves and synchrony in networks of oscillators of relaxation and non-relaxation type*, Phys. D, 89 (1995), pp. 169–183.
[37] B. van der Pol, *On "relaxation-oscillations,"* The London, Edinburgh, and Dublin Phil. Magazine and J. of Sci., 7 (1926), pp. 978–992.
[38] P. L. Varkonyi, T. Kiemel, K. Hoffman, A. H. Cohen, and P. Holmes, *On the derivation and tuning of phase oscillator models for lamprey central pattern generators*, J. Comput. Neurosci., in press.
[39] T. Wadden, J. Hellgren, A. Lansner, and S. Grillner, *Intersegmental coordination in the lamprey: Simulations using a network model without segmental boundaries*, Biol. Cybernet., 76 (1997), pp. 1–9.
[40] T. L. Williams, *Phase coupling by synaptic spread in chains of coupled neuronal oscillators*, Science, 258 (1992), pp. 662–665.
[41] T. L. Williams and K. A. Sigvardt, *Intersegmental phase lags in the lamprey spinal cord: Experimental confirmation of the existence of a boundary region*, J. Comput. Neurosci., 1 (1994), pp. 61–67.
[42] H. Wilson, *Spikes, Decisions and Actions: The Dynamical Foundations of Neuroscience*, Oxford University Press, Oxford, UK, 1999.
[43] A. T. Winfree, *The Geometry of Biological Time*, 2nd ed., Springer-Verlag, New York, 2001.